Application of white x-ray microbeams for the analysis of dislocation structures

R. I. Barabash,[a] G. E. Ice, B. C. Larson, and Wenge Yang
Metals and Ceramics and Solid State Divisions, Oak Ridge National Laboratory, Oak Ridge, Tennessee 37831-6118

(Presented on 22 August 2001)

The measurement of dislocation structures on mesoscopic length scales is a particularly important application of white-beam Laue microdiffraction. Near a Bragg reflection the intensity distribution in reciprocal space is sensitive to the organization of the dislocations, which occurs at several structural levels. Unpaired geometrically necessary dislocations (GND) and geometrically necessary boundaries (GNB) result in elongated streaks in the Laue image. The direction of the streaks depends on the average orientation of the dislocation arrays and the diffraction vectors. Laue images collected using synchrotron x-ray microbeams are sensitive to the detailed hierarchical distribution of dislocations and can be used to study the orientation and density of individual GNDs and GNBs.
© *2002 American Institute of Physics.* [DOI: 10.1063/1.1445830]

X-ray microbeam measurement of dislocation structures is an emerging new area. The techniques are based on classic polychromatic (white) beam Laue diffraction widely used to determine crystal symmetry and orientation. Compared with traditional monochromatic microbeam diffraction, the white-beam method has several advantages:[1–4] (1) the sample does not need to be rotated which allows rapid analysis of polycrystalline materials; (2) the intensity distributions around a large number of different reflections can be simultaneously measured and analyzed from the same subgrain; (3) an uncompromised full three-dimensional reciprocal space intensity distribution can be measured when necessary by scanning the incident beam energy.

Our analysis of dislocation structure is based on the general kinematic treatment of x-ray scattering from dislocations.[5–11] We restrict ourselves to the case where the intensity distribution is dominated by: (1) geometrically necessary boundaries (GNB) formed by tilt dislocations walls; and (2) hierarchy in dislocation structure with GNB separating regions with incidental dislocation boundaries (IDB) and individual geometrically necessary dislocations (GNDs) (Fig. 1). Treatment of white beam diffraction by unpaired individual GND is given in Ref. 12. In reciprocal space the exact positions of regular reflections (*hkl*) are related to the orientation and reciprocal space lattice distortions. The momentum transfer corresponding to a Bragg/Laue reflection $\mathbf{G}_{hkl}$ is defined by $\mathbf{k}_{hkl}-\mathbf{k}_0$, where $(|\mathbf{k}_0|=|\mathbf{k}_{hkl}|=k)$. Here $\mathbf{k}_0$ is the incident wave vector and $\mathbf{k}_{hkl}$ is the scattered wave vector that satisfies the Bragg/Laue conditions. The diffuse scattering intensity depends on the deviation $\mathbf{q}=\mathbf{Q}-\mathbf{G}_{hkl}=\mathbf{k}-\mathbf{k}_{hkl}$ between the diffraction vector $\mathbf{Q}=\mathbf{k}-\mathbf{k}_0$, and the momentum transfer $\mathbf{G}_{hkl}$ for a Laue reflection. The intensity distribution of a crystal with different dislocation arrays may be written as follows: [5,11,12]

$$I(\mathbf{q})=f^2\sum_{i,j} e^{i\mathbf{q}\mathbf{\Delta}}e^{-T}. \tag{1}$$

Here f is the average scattering factor of the matrix atoms; $\mathbf{\Delta}=\mathbf{R}_i^0-\mathbf{R}_j^0$ is the undistorted distance vector between the lattice cells i, j, and $T=nS\sum_t 1-e^{[i\mathbf{Q}(\mathbf{u}_{it}-\mathbf{u}_{jt})]}$ is the correlation function. Here S is the area of one dislocation in a transverse plane; n is the total dislocation density, and nS is a dimensionless quantity that indicates the fraction of lattice sites covered with dislocations. The total displacement of the ith cell $\mathbf{U}_i$ is calculated from a superposition of displacements $\mathbf{u}_{it}$ from all GNBs in the sample, $\mathbf{U}_i=\sum_t c_t\mathbf{u}_{it}$. Here $c_t=1$ if there is a GNB in the position t, and $c_t=0$ if there is no GNB at t.

Consider cells with different orientations in deformed material separated by GNBs formed by tilt dislocation walls

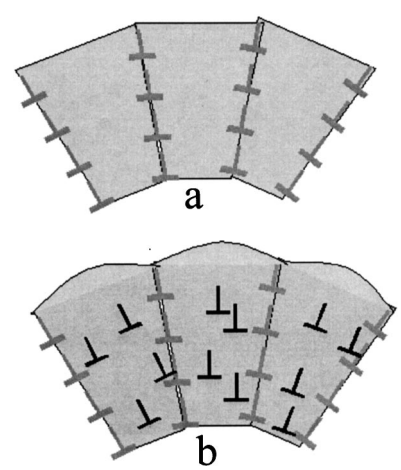

FIG. 1. Schematic of a crystal with different unpaired dislocations arrangements: (a) GNBs formed by tilt dislocation walls and (b) hierarchy of dislocation structures formed by GNBs and individual GNDs.

[a]Author to whom correspondence should be addressed; Electronic mail: barabashr@ornl.gov

 © 2002 American Institute of Physics

Downloaded 04 Sep 2009 to 160.91.157.167. Redistribution subject to AIP license or copyright; see http://rsi.aip.org/rsi/copyright.jsp

shown in Fig. 1(a). Each wall provides a rotation between two neighboring mosaic blocks around the direction of dislocation lines within the wall. The unit vector $\boldsymbol{\omega}$ parallel to the rotation axis of each wall coincides with the unit vector $\boldsymbol{\tau}$ along the dislocation lines in the case of a tilt boundary. We consider pure tilt boundaries formed by equidistant edge dislocations (so-called "thin walls"[13,14]). Such boundaries do not produce long-range strain, only rotations. The residual stresses in the boundary region are periodic with a wavelength $b^* = b \csc \Theta/2$. These stresses are appreciable only at the distances less then b^* from the boundary.[13] If h is the distance between these dislocations in the wall, one can consider the boundary as a single defect producing the local rotation field. The misorientation angle Θ due to such a boundary is defined by the equation $b/h = 2\sin(\Theta/2)$, where $b/h \approx \Theta$ for small angle boundaries.

To characterize this model quantitatively, we define the average size of the cells D_+ between the two neighboring GNBs and write the number of walls per unit length as $1/D^+$. The total density of unpaired dislocations grouped in the walls is denoted by $n^+ = 1/D^+ h$. The mean deformation tensor results in pure rotations about the direction of dislocation lines in the wall. This tensor depends on the type and misorientation angles of each GNB and their density.

Near a Laue spot, we can define two natural axes ξ and ν: $\xi = (\tau \times \mathbf{g})/(|\tau \times \mathbf{g}|)$, and $\nu = (\xi \times \mathbf{g})/(|\xi \times \mathbf{g}|)$ perpendicular to the momentum transfer unit vector $\mathbf{g}$. As in Ref. 12 with this coordinate system, the diffuse scattering is strongly elongated in the ξ direction. The full width at half maximum in the ξ direction, $\mathrm{FWHM}_\xi \propto (L\Theta/D^+) f(\hat{\tau}\hat{G}_{hkl})$, depends on the average distance between GNBs, their mutual orientation with the momentum transfer G, the type of GNB (tilt or twist), and the incident x-ray beam direction. In the second transverse direction ν, the $\mathrm{FWHM}_\nu \propto \Theta\sqrt{L/D}\,\varphi(\hat{\tau}\hat{G}_{hkl})$ depends on the total number of boundaries per unit length b/D and usually $\mathrm{FWHM}_\nu \ll \mathrm{FWHM}_\xi$. Here $f(\hat{\tau}\hat{G}_{hkl})$ and $\varphi(\hat{\tau}\hat{G}_{hkl})$ are orientation factors for the ξ and ν axes, L is the penetration depth, and D is the distance between any boundary [both GNDs and incidental dislocation boundaries (IDBs)]. Correlations in the positions of GNBs may change the value of the orientation factor. Along the direction of dislocation lines within the wall, the width of the reciprocal space intensity distribution is of the order $\delta q_\omega \sim 2\pi/L_\omega$, where L_ω is the size of the crystal or a subgrain in the direction of the dislocation line.

We simulated the intensity of scattering by crystals with two model fragments as shown in Fig. 2. Each fragment has a size of 2500 interatomic spacing. The total value of unpaired dislocations was kept constant. A total density of individual unpaired dislocation $n^+ = 10^{12}$ cm^{-2} was chosen typical of highly deformed crystals. To initiate the simulation we randomly distributed all dislocations. The contour map has a huge broadening along the ξ axis with a typical "flat-top" shape [Fig. 2(a)]. As dislocations are removed from the fragments and added to a common GNB, a correlated misorientation develops between the two parts of the crystal. For distance between dislocations inside the wall of approximately 21 interatomic spacings, a rotation of about $\Theta \approx 2^0$

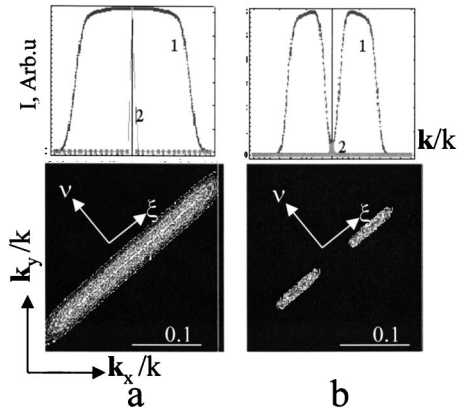

FIG. 2. Splitting of Laue spots resulting from grouping of a number of individual GNDs into a single GNB: simulated intensity distributions and contour maps in ξ–ν plane for white beam Laue scattering by a crystal with a dislocation hierarchy along the ξ (1) and ν (2) axes for the (222) reflection (total number of dislocations in the boundary and randomly distributed inside the fragments is constant). Size of the crystal $L = 2500d$: (a) crystal with random individual GNDs, $n^+ = 10^{12}$ cm^{-2} ($K<1$) and (b) two separate streaks due to the formation of random GNDs $n^+ = 4\times10^{10}$ cm^{-2} and one GNB ($K>1$).

occurs between the two fragments (cells). This reduces the density of random individual dislocations inside each fragment to $n^+ = 2\times10^{11}$ cm^{-2}. The intensity distribution changes as shown in the flat-top intensity distribution along the ξ axis. Further grouping into the wall results in splitting of the reflection into two separate streaks [Fig. 2(b)]. This splitting is observed when density of random GNDs reduces to $n^+ = 4\times10^{10}$ cm^{-2} and $\Theta \approx 2.12^0$.

To understand this splitting, let us assume that along the penetration depth L the x-ray beam intersects several fragments with average size D^+ separated with GNBs. Each fragment contributes to the diffraction. The number of such contributions is equal to L/D^+. Each GNB produces an average misorientation Θ. The average distance between the Laue maximums formed by two adjacent fragments is $\Delta = (Q/k_0)\Theta$. If this distance exceeds the average $\mathrm{FWHM}_{\mathrm{fr}}$ of the Laue image for each fragment along the ξ axis, splitting of the Laue spot will occur. For a hierarchy structure with GNBs and GNDs, the following criterion can be used: $K = (\Theta Q/k_0 \mathrm{FWHM}_{\mathrm{fr}})$. If $K<1$, the intensity distribution of a white beam reflection is continuous; if $K>1$ this reflection is split into separate spots. Scattering from GNDs contributes to the $\mathrm{FWHM}_{\mathrm{fr}}$.

Unpaired individual and boundary dislocations influence Laue scattering differently. Both unpaired GNBs and individual GNDs result in a total macroscopic lattice rotation of the crystal and cause streaking. Due to local strains, however, individual GNDs influence the length of the streak more than the same number of dislocations in a boundary. Moreover, the FWHM, in the narrow direction of the streak, is most strongly influenced by individual GNDs and can possibly be used to separate boundary dislocations from the ones inside the fragment. The $\mathrm{FWHM}_{\mathrm{fr}}$ depends on the density of GNDs and on the experimental resolution function. For

Downloaded 04 Sep 2009 to 160.91.157.167. Redistribution subject to AIP license or copyright; see http://rsi.aip.org/rsi/copyright.jsp

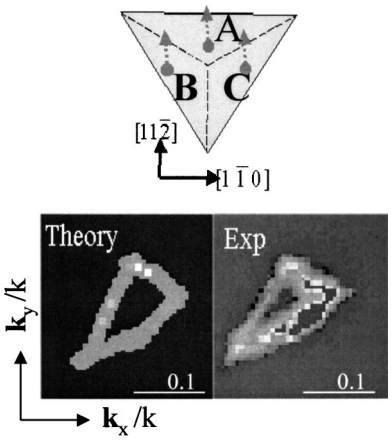

FIG. 3. Laue images reveal which GND and GNBs are operative in the material under the indentation. The following dislocations systems were used to model Laue images for position B in the indentation: (1) $\hat{\tau}||[101]$, $\hat{b}||[10\bar{1}]$; (2) $\hat{\tau}||[\bar{1}2\bar{1}]$, $\hat{b}||[101]$; (3) $\hat{\tau}||[\bar{1}1\bar{2}]$, $\hat{b}||[110]$; (4) $\hat{\tau}||[1\bar{1}\bar{2}]$, $\hat{b}||[110]$; and (5) $\hat{\tau}||[\bar{2}\bar{1}1]$, $\hat{b}||[011]$.

higher resolution measurements, a larger number of separate spots can be detected within a streak as observed experimentally.

We applied this microbeam-Laue technique to a complicated heterogeneous dislocation structure arising from plastic deformation in a nanoindented Cu single crystal. The Cu single crystal surface normal was parallel to [111], and the upper side of the pyramidal nanoindent is almost parallel to $[1\bar{1}0]$ (Fig. 3). Laue images were taken at various positions in and near the pyramidal nanoindent crater. Both the experimental data and the model images reveal long streaks with distinctive orientations that can abruptly change direction. A simple image (uniaxial elongated streak) obtained for position A was discussed previously.[2,12] Images taken at positions B and C are more complicated. Experimental and simulated images taken in position B are shown in Fig. 3. The x-ray beam intersects several fragments with qualitatively different dislocation structures. The plastic response to indentation can be understood by the formation of GNBs separating cells rotated by the deformation and individual GNDs, both of which appear in the material to accommodate the indent volume.[15] To model the image in position B, we needed at least five different fragments separated by GNBs. Each fragment had a different orientation and density of GNDs. These fragments (cells) had different sizes along the beam and were rotated relative to each other by GNBs. These were used as fitting parameters during the simulation.

In summary, we have developed a method for calculating the white-beam Laue diffraction pattern from simple dislocation distributions in a crystal. This approach can be used to estimate the type, orientation, and density distribution of individual GNDs and GNBs in deformed materials.

This research was sponsored by the Division of Materials Sciences and Engineering, Office of Basic Energy Sciences, U. S. Department of Energy, under Contract No. DE-AC05-00OR22725 with UT-Battelle, LLC.[16] Work performed in part on MHATT-CAT beamline 7 at the APS. MHATT-CAT sector is supported in part by DOE Grant No. DE-FG02-99ER45743.

[1] G. E. Ice, X-Ray Spectrom. **26**, 315 (1997).
[2] B. C. Larson, N. Tamura, J. S. Chung, G. Ice, J. D. Budai, J. Z. Tischler, W. Yang, H. Weiland, and W. P. Lowe, Mater. Res. Soc. Symp. Proc. **590**, 247 (2000).
[3] M. A. Marcus, A. A. Macdowell, E. D. Isaacs, K. Evans-Lutterodt, and G. Ice, Mater. Res. Soc. Symp. Proc. **428**, 545 (1996).
[4] J. S. Chung, N. Tamura, G. Ice, B. C. Larson, and J. D. Budai, Mater. Res. Soc. Symp. Proc. **563**, 169 (1999).
[5] M. Krivoglaz, *X-ray and Neutron Diffraction in Nonideal Crystals* (Springer, Berlin, 1996).
[6] B. Warren, *X-ray Diffraction* (Dover, New York, 1969).
[7] M. Wilkens, Phys. Status Solidi A **2**, 359 (1970); *Fundamental Aspects of Dislocation Theory II*, edited by J. A. Simmons, R. de Wit, and R. Bullough, National Bureau of Standards Special Publication 317, (National Bureau of Standards, Washington, 1970), pp. K1–K7.
[8] R. Thomson and L. Levine, Acta Crystallogr., Sect. A: Found. Crystallogr. **53**, 590 (1997).
[9] T. Ungar, H. Mughrabi, D. Ronnpagel, and M. Wilkens, Acta Metall. **32**, 333 (1984).
[10] S. N. G. Chu, A. T. Macrander, K. E. Strege, and W. D. Johnston, J. Appl. Phys. **57**, 249 (1985).
[11] R. Barabash and P. Klimanek, J. Appl. Crystallogr. **32**, 1050 (1999).
[12] R. Barabash, G. E. Ice, B. C. Larson, G. M. Pharr, K.-S. Chung, and W. Yang, Appl. Phys. Lett. **79**, 4 (2001).
[13] F. R. N. Nabarro, *Theory of Crystal Dislocations* (Dover, New York, 1987).
[14] D. Hughes and N. Hansen, Acta Mater. **48**, 2985 (2000).
[15] A. Gouldstone, H.-J. Koh, A. E. Giannakopulus, and S. Suresh, Acta Mater. **48**, 2277 (2000).
[16] The submitted manuscript has been authored by a contractor of the U.S. Government under Contract No. DE-AC05-00OR22725. Accordingly, the U.S. Government retains a nonexclusive, royalty-free license to publish or reproduce the Published form of this contribution, or allow others to do so, for U.S. Government purposes.

Downloaded 04 Sep 2009 to 160.91.157.167. Redistribution subject to AIP license or copyright; see http://rsi.aip.org/rsi/copyright.jsp